Mixed-Valence Class I Transition and Electrochemistry of Bis(triphenylamine)-Based Aramids Containing Isolated Ether-Linkage

HUNG-JU YEN,[1] SHIUE-MING GUO,[1] GUEY-SHENG LIOU,[1] JEN-CHIEH CHUNG,[2] YU-CHANG LIU,[2] YUNG-FANG LU,[2] YU-ZHEN ZENG[2]

[1]Functional Polymeric Materials Laboratory, Institute of Polymer Science and Engineering, National Taiwan University, 1 Roosevelt Road, 4th Sec., Taipei 10617, Taiwan

[2]Institute of Nuclear Energy Research, Atomic Energy Council, No. 1000, Wenhua Rd., Jiaan Village, Longtan Township, Taoyuan County 32546, Taiwan

Received 16 May 2011; accepted 1 June 2011
DOI: 10.1002/pola.24819
Published online 7 July 2011 in Wiley Online Library (wileyonlinelibrary.com).

ABSTRACT: A series of solution-processable electrochromic (EC) aromatic polyamides with bis(triphenylamine)ether (TPAO) units in the backbone were prepared by the phosphorylation polyamidation from a newly synthesized diamine monomer, bis(*N*-4-aminophenyl-*N*-4-methoxyphenyl-4-aminophenyl)ether, and various dicarboxylic acids. These polymers were highly soluble in many organic solvents and showed useful levels of thermal stability associated with high glass-transition temperatures and high char yields (higher than 50 at 800 °C in nitrogen). The polymer films showed reversible electrochemical oxidation and electrochromism with high contrast ratio in the visible range, which also exhibited moderate coloration efficiency (CE), low switching time, and good stability. Especially, the polyamides with two electroactive nitrogen centers only showed one-stage oxidative coloring (no intervalence charge-transfer [IV-CT] band was detected), implying the two electrons are simultaneously removed from the TPAO units on account of the ether-linkage definitely isolated the two redox centers. The mixed-valence (MV) Class I/II/III transition and electrochemistry of the synthesized model compounds were investigated for the bridged triarylamine system with various N—N distances and intramolecular electron transfer (ET) capability. © 2011 Wiley Periodicals, Inc. J Polym Sci Part A: Polym Chem 49: 3805–3816, 2011

KEYWORDS: electrochemistry; high performance polymers; polyamides; polycondensation

INTRODUCTION Electrochromism involves electroactive materials that present a reversible change in optical properties when the material is electrochemically oxidized or reduced.[1] Recently, electrochromic (EC) utilization, such as antiglare back mirrors, smart windows, and E-papers has already been commercialized.[2] In general, most applications require EC materials with a high contrast ratio ($\Delta T\%$), coloration efficiency (CE), cycle life, and rapid response time. EC materials, such as transition-metal oxides, inorganic coordination complexes, conjugated polymers, and organic molecules, have been directed from optical changes in the visible-light (e.g., 400–800 nm) to the near infrared (NIR; e.g., 800–2000 nm) regions increasingly.[3] According to Robin and Day,[4] the *p*-phenylenediamine-containing molecule is an interesting anodic EC system for NIR applications due to its particular intramolecular electron transfer (ET) in the oxidized states.

Intramolecular ET processes have been studied extensively in the mixed-valence (MV) systems.[5] They usually used one-dimensional MV compounds containing two or more redox states connected via saturated or unsaturated molecule. MV systems can be classified into three categories:[4] Class I with practically no coupling between the different redox states, Class II with moderate electronic coupling, and Class III with strong electronic coupling (the electron is delocalized over the two redox centers). In recent experimental and theoretical studies,[6] the *N*,*N*,*N*′,*N*′-tetraphenyl-*p*-phenylenediamine (TPPA) cation radical has been reported as a symmetrical delocalized Class III structure with a strong electronic coupling, whereas *N*,*N*,*N*′,*N*′-tetraphenylbenzidine (TPB) cation radical was demonstrated as a Class II structure with a weakly electronic coupling. Among the numerous redox centers, triarylamine system is of great interest of investigating hole-transfer processes between redox centers. In early research, the MV character of bis(triarylamine) derivatives with varying π-electron spacers has been investigated. The distances of triarylamine redox centers vary from 0.5 to 2 nm. All radical cation species show rather strong intervalence charge-transfer (IV-CT) bands in the NIR region.[7] In our laboratory, we also have systemically developed TPPA and TPB-containing aromatic polyamides,[8] which revealed

Additional Supporting Information may be found in the online version of this article. Correspondence to: G.-S. Liou (E-mail: gsliou@ntu.edu.tw)
Journal of Polymer Science Part A: Polymer Chemistry, Vol. 49, 3805–3816 (2011)

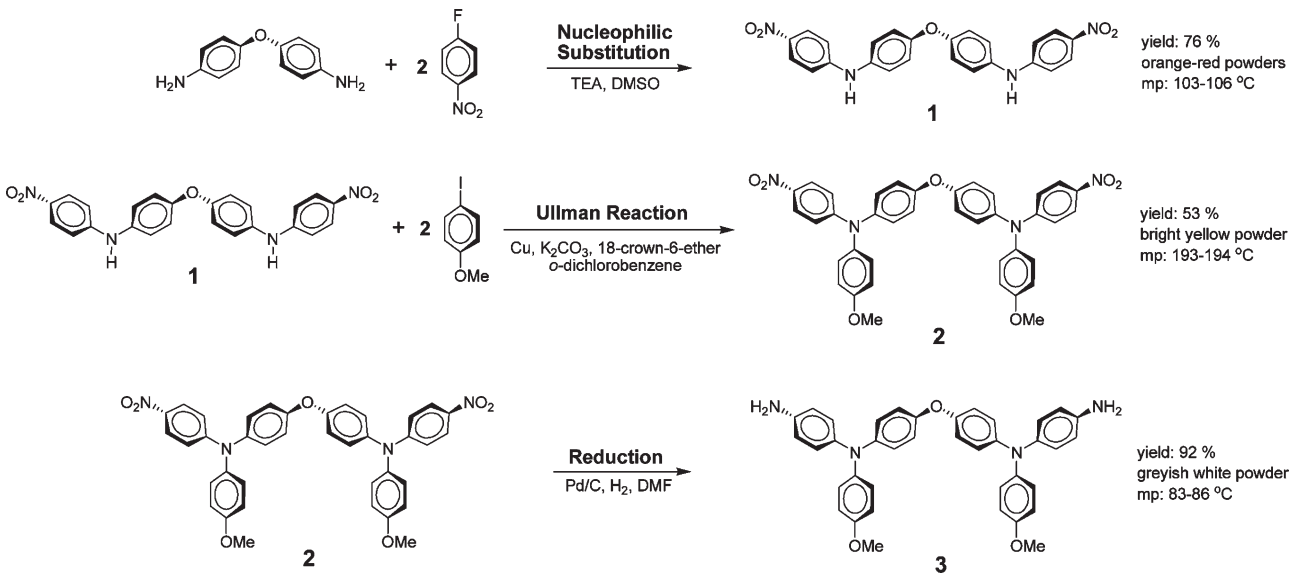

SCHEME 1 Monomer synthesis.

typical Class III and II transitions in MV systems, respectively.

Therefore, our strategy of this work is to design and synthesize bis(triphenylamine)ether (TPAO)-based EC polymers with a ether-linkage between two electroactive nitrogen centers. The MV Class I character and behavior would be obtained in the resultant electroactive polymers by using the ether-linkage as a block and definitely isolated the two redox centers. These electroactive polymers with high molecular weights and excellent thermal stability should be readily prepared by using conventional polycondensation.[9] Because of the incorporation of packing-disruptive TPAO units into the polymer backbone, these novel polymers should also have excellent solubility in various polar organic solvents; thus, transparent and flexible polymer thin films could be easily prepared by solution-casting and spin-coating techniques. This is beneficial for their fabrication of large-area, thin-film EC devices.

In this contribution, we therefore synthesized the diamine monomer, bis(*N*-4-aminophenyl-*N*-4-methoxyphenyl-4-aminophenyl)ether (**3**), and its derived aromatic polyamides containing ether-linkage in the main chain with *para*-substituted methoxy groups. In addition to the general properties (such as inherent viscosities, solubility, and thermal properties), the electrochemical and EC behaviors of these polymers were also investigated. To demonstrate that the NIR absorbance and MV system could be adjusted by the distance between two electroactive nitrogen redox centers, electrochemistry and spectroelectrochemistry of the corresponding model compounds **M1**, **M2**, and **2** were investigated and discussed herein.

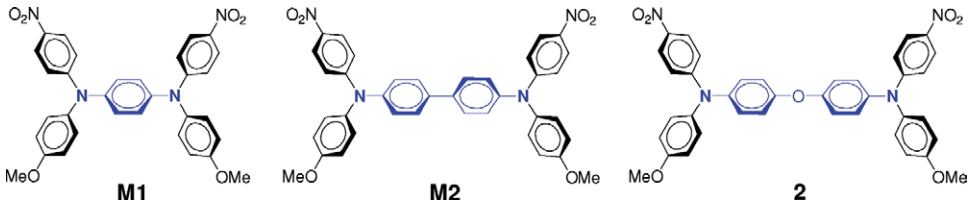

RESULTS AND DISCUSSION

Monomer Synthesis

The new aromatic diamine bis(*N*-4-aminophenyl-*N*-4-methoxyphenyl-4-aminophenyl)ether (**3**) was synthesized by hydrogen Pd/C-catalyzed reduction of the dinitro compound bis(*N*-4-methoxyphenyl-*N*-4-nitrophenyl-4-aminophenyl)ether (**2**) resulting from the potassium carbonate-mediated aromatic nucleophilic substitution reaction of bis(*N*-4-nitrophenyl-4-aminophenyl)ether with 4-iodoanisole (Scheme 1). Elemental analysis, Fourier transform infrared (FTIR), and NMR measurements were used to identify structures of the intermediate compound (**1**), dinitro compound (**2**), and the target diamine monomer (**3**). The FTIR spectra of these three synthesized compounds are illustrated in Supporting Information Figure S1. The nitro groups of compound **2** exhibited two characteristic bands at around 1586 and 1314 cm^{-1} due to nitro asymmetric and symmetric stretching. After reduced to diamine monomer (**3**), the characteristic absorption bands of the nitro group disappeared and the primary amino group showed the typical absorption pair at 3443 and

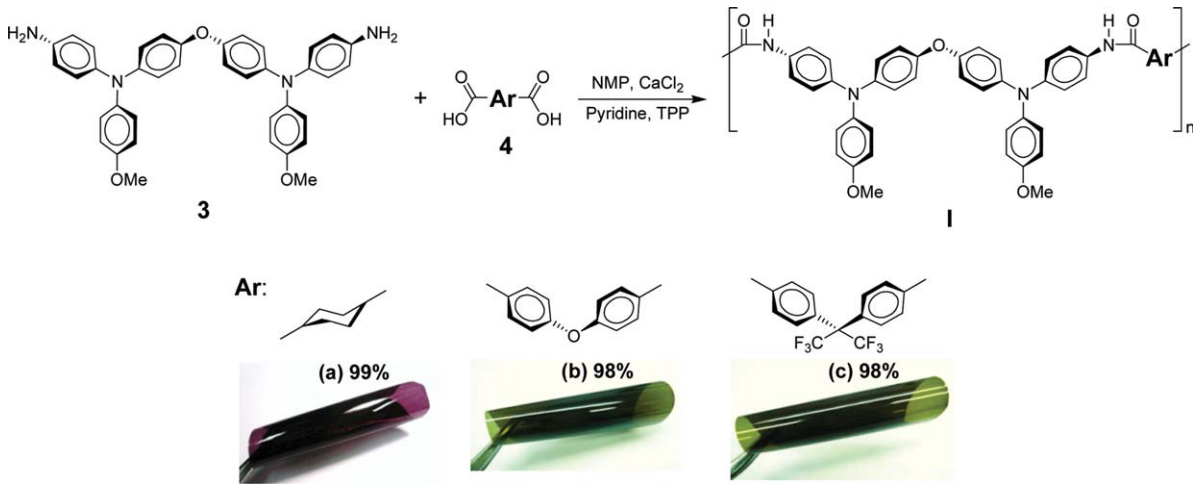

SCHEME 2 Synthesis of polyamides by direct polycondensation reaction (60–80 μm). [Color figure can be viewed in the online issue, which is available at wileyonlinelibrary.com.]

3365 cm^{-1} (N—H stretching). ^{1}H, ^{13}C, H—H COSY, and C—H HMQC NMR spectra of the compounds **1–3** are illustrated in Supporting Information Figures S2–S6 and agree well with the proposed molecular structures. The ^{1}H NMR spectra confirm that the nitro groups have been completely transformed into amino groups by the high field shift of the aromatic protons and the resonance signals at around 4.96 ppm corresponding to the amino protons.

Polymer Synthesis

According to the phosphorylation technique first described by Yamazaki et al.,[10] a series of novel polyamides (**Ia–Ic**) with TPAO units in the backbone were synthesized from the diamine (**3**) and various dicarboxylic acids via solution polycondensation using triphenyl phosphite and pyridine as condensing agents (Scheme 2). All the polymerization proceeded homogeneously throughout the reaction and afforded clear and highly viscous polymer solutions, which formed a tough, fiberlike precipitate when slowly poured into stirring methanol. The obtained polyamides had inherent viscosities in the range of 0.43–0.63 dL/g with number-average molecular weights (M_n) and polydispersity (PDI) of 109,000–151,200 Da and 1.76–1.81, respectively, relative to polystyrene standards (Supporting Information Table S1) and could be solution cast into flexible and tough films. The appearance and quality of these films are also shown in Scheme 2. The formation of polyamides was also confirmed by IR and NMR spectroscopy. Supporting Information Figure S7 exhibits a typical IR spectrum for polyamide **Ib**. The characteristic IR absorption bands of the amide group were around 3317 (N—H stretching) and 1649 cm^{-1} (amide carbonyl). Supporting Information Figure S8 depicts a typical set of ^{1}H and ^{13}C spectra of polyamide **Ib** in dimethyl sulfoxide-d_6 (DMSO-d_6); all the peaks could be readily assigned to the hydrogen atoms of the recurring unit. The resonance peak appearing at 10.15 ppm in the ^{1}H NMR spectrum supports the formation of amide linkages. The structurally related polyamide **I′b** shown in Table 1 is used for comparison studies and the synthesis and characterization have been described previously.[11]

Solubility and Film Property

The solubility behavior of polymers **Ia–Ic** was investigated and the results are also listed in Supporting Information Table S2. Most of the polyamides were readily soluble in polar aprotic organic solvents such as *N*-methyl-2-pyrrolidinone (NMP), *N*,*N*-dimethylacetamide (DMAc), *N*,*N*-dimethylformamide (DMF), and *m*-cresol. Thus, the excellent solubility makes these polymers as potential candidates for practical applications by spin-coating or inkjet-printing processes to afford high performance thin films for optoelectronic devices. As mentioned earlier, the polyamides **Ia–Ic** could be solution cast into flexible, transparent, and tough films. Their high solubility

TABLE 1 Redox Potentials and Energy Levels of Polyamides

	Thin Film (nm)		Oxidation Potential (V)[a]					
Code	λ_{max}	λ_{onset}	$E^{ox}_{p,an}$	$E^{ox}_{p,ca}$	E_{onset}	E_g (eV)[b]	HOMO (eV)[c]	LUMO (eV)
Ia	312	366	1.00	0.66	0.67	3.39	5.11	1.72
Ib	313	400	1.02	0.66	0.69	3.10	5.13	2.03
Ic	306	407	1.03	0.69	0.71	3.05	5.15	2.10
I′b	345	407	0.94	0.58	0.65	3.05	5.06	2.01

[a] From cyclic voltammograms versus Ag/AgCl in CH_3CN.
[b] The data were calculated from polymer films by the equation: $E_g = 1240/\lambda_{onset}$ (energy gap between HOMO and LUMO).
[c] The HOMO energy levels were calculated from cyclic voltammetry and were referenced to ferrocene (4.8 eV; onset = 0.36 V).

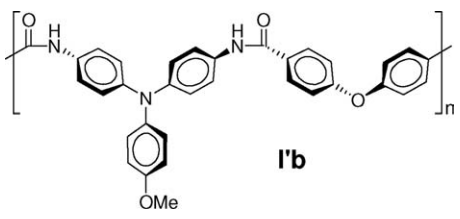

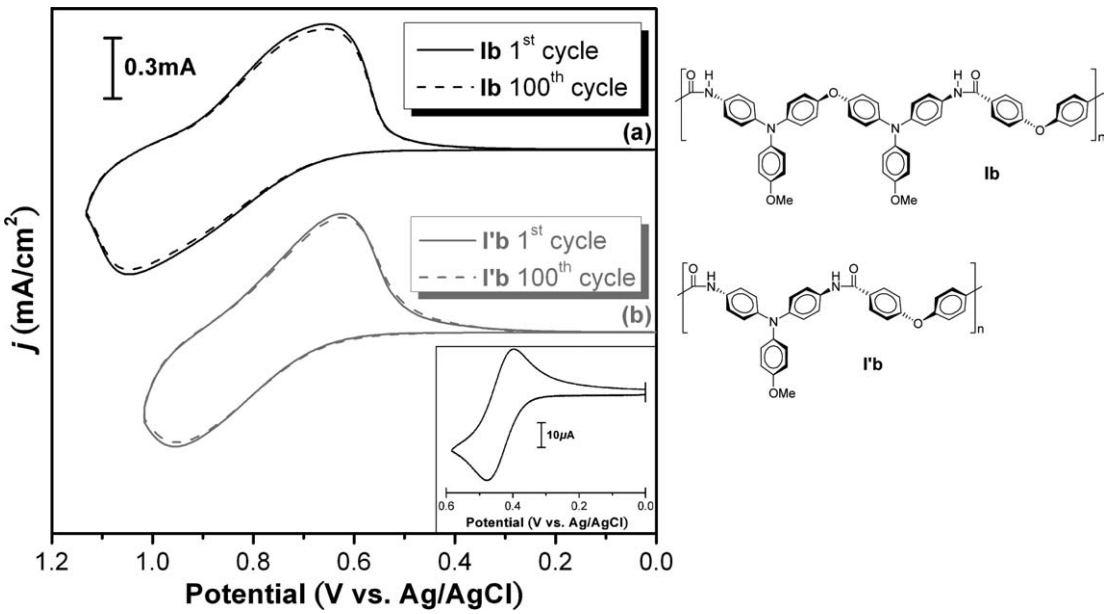

FIGURE 1 Cyclic voltammetric diagrams of polyamide (a) **Ib** and (b) **I′b** films on an ITO-coated glass substrate over cyclic scans and ferrocene (inset) in 0.1 M TBAP/CH_3CN at a scan rate of 50 mV/s.

and amorphous nature can be attributed to the incorporation of bulky, three-dimensional (3D) TPAO moiety along the polymer backbone, which results in a high steric hindrance for close packing thus reduces their crystallization tendency.

Thermal Properties

The thermal properties of the polyamides were investigated by thermogravimetric analysis (TGA) and differential scanning calorimetry (DSC) and are summarized in Supporting Information Table S3. Typical TGA curves of representative polyamide **Ib** in both air and nitrogen atmospheres are shown in Supporting Information Figure S9. All the aromatic polyamides exhibited good thermal stability with insignificant weight loss up to 440 °C in nitrogen. Their 10% weight-loss temperatures in nitrogen and air were recorded at 465–520 and 475–525 °C, respectively. The carbonized residue (char yield) of these aromatic polymers was more than 53% at 800 °C in nitrogen atmosphere. The high char yields of these polymers could be ascribed to their high aromatic content. The glass-transition temperature (T_g) could be easily measured by the DSC thermograms; they were observed in the range of 258–265 °C as shown in Supporting Information Figure S10, depending on the stiffness of the polymer chain. All the polymers indicated no clear melting endotherms up to the decomposition temperatures on the DSC thermograms, which supports the amorphous nature of these polyamides.

Electrochemical Properties

The electrochemical behavior of the polyamides was investigated by cyclic voltammetry (CV) conducted by film cast on an ITO-coated glass substrate as the working electrode in dry acetonitrile (CH_3CN) containing 0.1 M of tetrabutylammonium perchlorate (TBAP) as an electrolyte. The typical CVs for polyamides **Ib** and **I′b** are shown in Figure 1 for comparison. The polyamide **Ib** [with $(OMe)_2$TPAO units] having two electroactive nitrogen centers revealed only one reversible oxidation redox (E_{onset} = 0.69 V), implying that two electrons are almost simultaneously removed from the two definitely separated triarylamine units with independent behavior, to form two radical cations on account of the block of ether-linkage between the two redox centers, which is similar to **I′b** [with (OMe)TPA units]. The lower oxidation potential of polymer **I′b** (E_{onset} = 0.65 V) could be attributable to the electron-donating methoxy- and amino-substituents at the *para*-position of phenyl rings. After hundred continuous cyclic scans between 0.00 and 1.13 V, the polymer films still exhibited good electrochemical stability.

The other polyamides (**Ia** and **Ic**) showed similar CV curves to that of **Ib**. The redox potentials of the polyamides as well as their respective highest occupied molecular orbital (HOMO) and lowest unoccupied molecular orbital (LUMO; vs. vacuum) are summarized in Table 1. The HOMO level or called ionization potentials (vs. vacuum) of polyamides **Ia**–**Ic** are estimated from the onset of their oxidation in CV experiments as 5.11–5.15 eV (on the basis that ferrocene/ferrocenium is 4.8 eV below the vacuum level with E_{onset} = 0.36 V).

Figures 2 and 3 show CV and differential pulse voltammetry (DPV) of the model compounds **M1**, **M2**, and **2**, and the results are summarized in Table 2. For comparison, all measurements of model compounds were obtained under the same conditions. In CV scans (Fig. 2), we observed two reversible oxidation redox steps for **M1** ($E^{ox,1}_{p,an}$ = 0.93 V and $E^{ox,2}_{p,an}$ = 1.15 V), and only one reversible oxidation redox step for **M2** ($E^{ox}_{p,an}$ = 1.07 V) and **2** ($E^{ox}_{p,an}$ = 1.16 V), respectively, indicating the effect of N—N distance between two redox center on oxidation potential and intramolecular ET process. In addition, DPV diagrams of these model compounds (Fig. 3) also display two one-electron oxidation redox for **M1**

and only one two-electron oxidation redox for both **M2** and **2**, respectively. Because of the lack or absence of electrochemical splitting, neither electrostatic effects nor electron coupling could be observed for both **M2** and **2** in CV and DPV; the further investigation was performed by spectroelectrochemical measurements.

Measurement of *n* Electrons Transferred for Each Step of Model Compounds

Spectroelectrochemistry of model compounds[12] was examined by an optically transparent thin-layer electrode (OTTLE) coupled with UV–vis–NIR spectroscopy. The concentration of 5×10^{-4} M CH_3CN solution was prepared and a 100-mesh platinum film was used as a working electrode. To measure the amount of n electrons transferred for each step by the OTTLE techniques, a series of potentials ($E_{applied}$) are sequentially impressed (potentiostated) across the transparent cell containing a solution of the redox couple. At each applied potential, the ratio of the concentrations of oxidized form to neutral one, [O]/[N], of the couple adjusts by electrolysis at the transparent electrode to the value required for adherence to the Nernst equation:

$$E_{applied} = E^{\circ} + \frac{0.059}{n} \log \frac{[O]}{[N]}$$

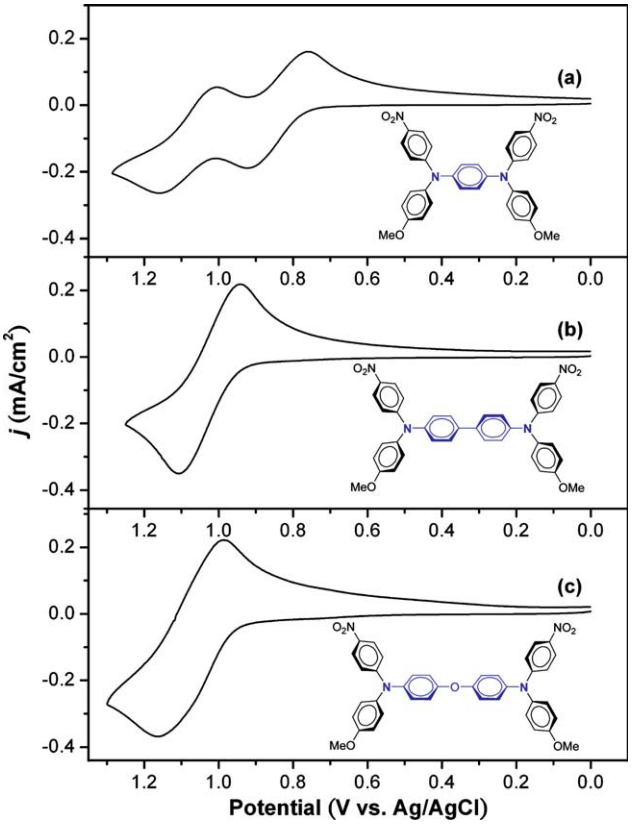

FIGURE 2 Cyclic voltammetric diagrams of 10^{-3} M model compounds (a) **M1**, (b) **M2**, and (c) **2** in 0.1 M TBAP/CH_3CN at a scan rate of 50 mV/s. [Color figure can be viewed in the online issue, which is available at wileyonlinelibrary.com.]

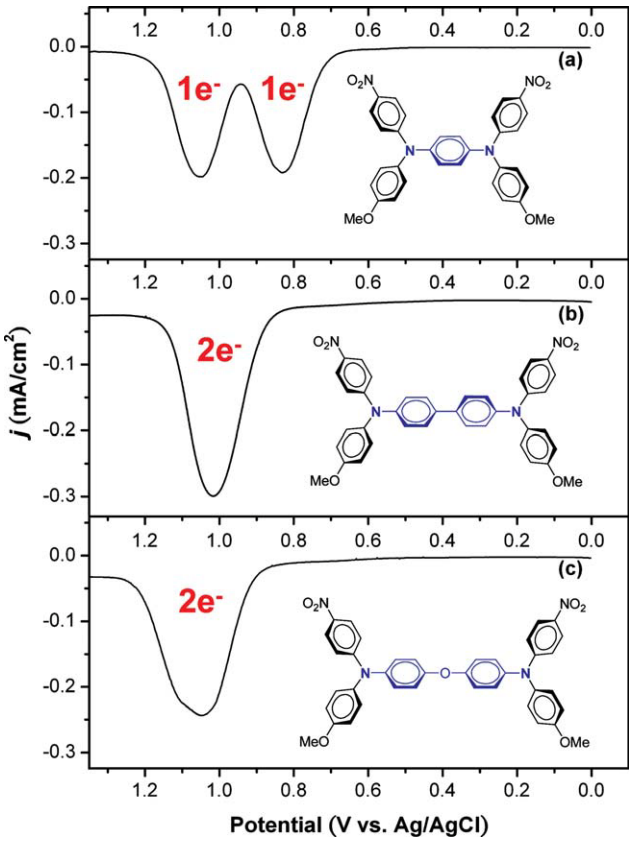

FIGURE 3 Differential pulse voltammetric diagrams of model compounds (a) **M1**, (b) **M2**, and (c) **2** (10^{-3} M) in 0.1 M TBAP/CH_3CN at a scan rate of 50 mV/s. [Color figure can be viewed in the online issue, which is available at wileyonlinelibrary.com.]

where E^{o} is a formal oxidation potential. Each applied potential is maintained until the equilibrium value of [O]/[N] has been established throughout the thin layer of solution adjacent to the platinum film electrode by electrolysis and diffusion. The optical transparency of the electrode enables the [O]/[N] value corresponding to each $E_{applied}$ to be obtained from absorbance changes measured by recording spectra directly through the transparent electrode and the thin layer of solution after equilibrium is achieved for each potential.

Figures 4–6 depict the spectral changes for model compounds **M1**, **M2**, and **2** at various electrode potentials. **M1** is

TABLE 2 Electrochemical Properties of Model Compounds **M1**, **M2**, and **2**

	Oxidation (V; vs. Ag/AgCl in CH_3CN)[a]				
Code	$E^{ox,1}_{p,an}$	$E^{ox,1}_{p,ca}$	E_{onset}	$E^{ox,}_{p,an}$	$E^{ox,2}_{p,ca}$
M1	0.93 ($1e^-$)	0.77	0.79	1.15 ($1e^-$)	1.01
M2	1.07 ($2e^-$)	0.91	0.93	–	–
2	1.16 ($2e^-$)	0.98	0.98	–	–

[a] From cyclic voltammograms versus Ag/AgCl in CH_3CN.
[b] $1e^-$ = one-ET, $2e^-$ = two-ET; calculated from the integral of the DPV.

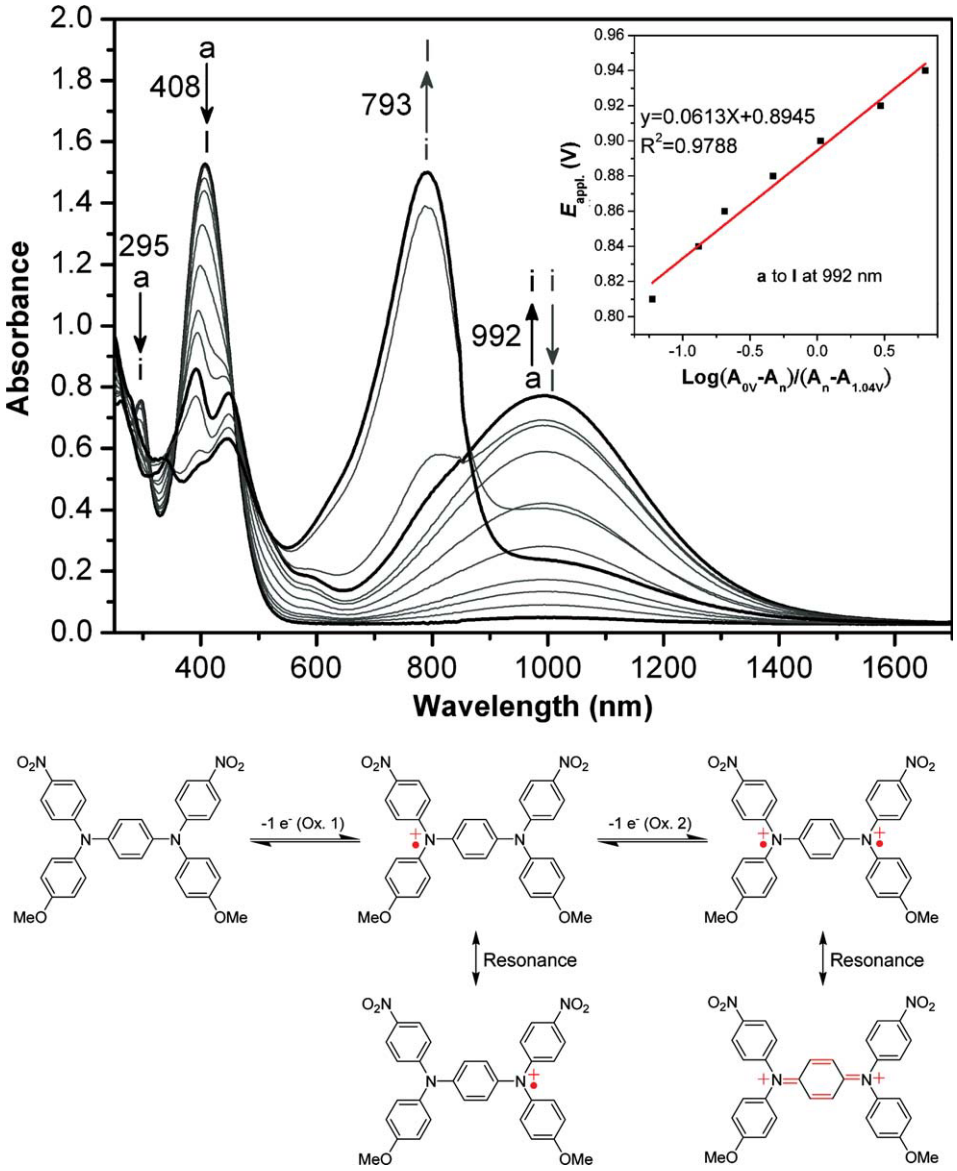

FIGURE 4 Absorption spectral change of compound **M1** (5×10^{-4} M) in 0.1 M TBAP/CH_3CN at $E_{applied}$ of (a) 0, (b) 0.81, (c) 0.84, (d) 0.86, (e) 0.88, (f) 0.90, (g) 0.92, (h) 0.94, (i) 1.00, (j) 1.03, (k) 1.06, and (l) 1.13 (V vs. Ag/AgCl) and the oxidation pathway. [Color figure can be viewed in the online issue, which is available at wileyonlinelibrary.com.]

used as an example to illustrate how many electrons are transferred for each step. The absorption peaks at 295 and 408 nm are characteristic for **M1** (Fig. 4). After first stage of one-electron oxidation (0.00–1.00 V), the original peaks decreased gradually, and a broad and intense new band around 992 nm appeared. When the potential was adjusted to more positive values (1.00–1.13 V) corresponding to the second stage of one-electron oxidation, the new peak appeared at 793 nm. The spectral change of **M1** was consistent with the reported MV Class III transition.[7] The inset in Figure 4 shows a typical plot of $E_{applied}$ versus $\log(A_n - A_0)/(A_f - A_n)$ corresponding to 992 nm (IV-CT band of Class III) for the first oxidized stage. The color of compound **M1** solution switches from brown (neutral state) to green (semioxidized state) and blue (fully oxidized state). The slope of the straight-line plot is 61.3 mV, which compares favorably with the Nernstian value of 59.1 mV for a one-electron process. The potential-axis intercept is 0.89 V, which is in good agreement with values of 0.85 V obtained by CV. Other model compounds **M2** and **2** revealed slopes of 62.9 mV for one-electron process and 38.0 mV for two-electron process. In Figure 5, owing a broad IV-CT characteristic band around 1367 nm from the cation radical state, compound **M2** could be claimed as the Class II system, and the color of compound **M2** solution switches from brown (neutral state) to red (semioxidized state) and blue (fully oxidized state).[7] For compound **2**, the introduction of ether-linkage definitely separated two redox centers with independent behavior, and the two electrons on TPAO units are simultaneously removed to form two radical cations. Furthermore, no IV-CT band could be detected in Figure 6 during oxidation, indicating that there is no stable single radical cation existing in TPAO units, and these two triarylamine in TPAO units should be oxidized at the same time with a color switches from light-brown (neutral state) to bluish-green (oxidized state) of the solution. The result suggests that the introduction of ether-

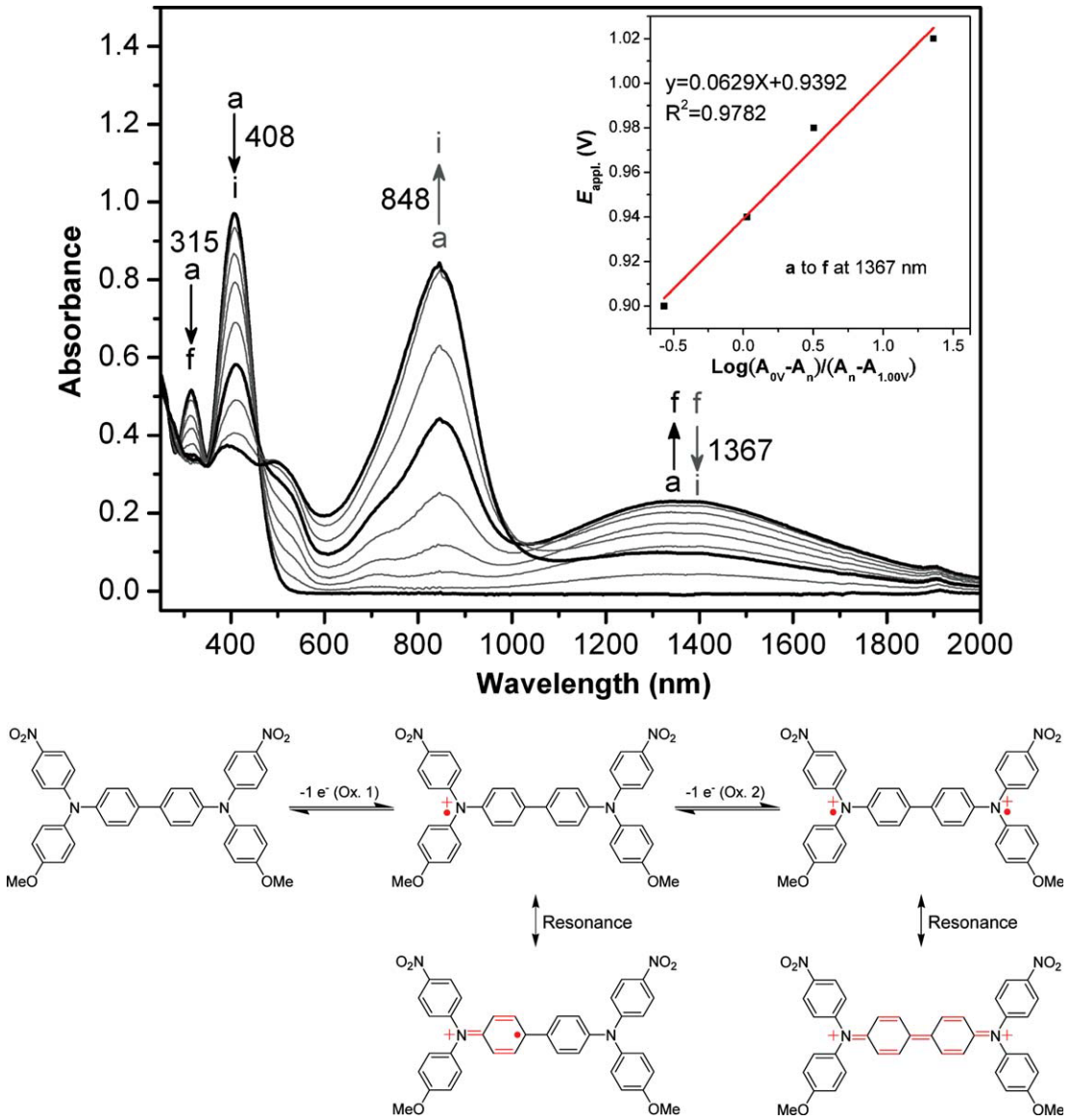

FIGURE 5 Absorption spectral change of compound **M2** (5×10^{-4} M) in 0.1 M TBAP/CH_3CN at $E_{applied}$ of (a) 0, (b) 0.90, (c) 0.94, (d) 0.98, (e) 1.02, (f) 1.04, (g) 1.06, (h) 1.09, and (i) 1.14 (V vs. Ag/AgCl) and the oxidation pathway. [Color figure can be viewed in the online issue, which is available at wileyonlinelibrary.com.]

linkage is an effective method for the purpose of tuning the Class I/II transition.

Spectroelectrochemical and EC Properties

Electrochromism of the polyamide thin films was examined by an OTTLE coupled with UV–vis–NIR spectroscopy. The preparation of electrode and solution was identical to those used in CV. UV–vis–NIR absorbance curves corresponding to applied potentials and 3D transmittance–wavelength–applied potential correlation of **Ib** film are depicted in Figure 7 and Supporting Information Figure S11. The peak of absorption at 314 nm, characteristic for the neutral form of polyamide **Ib**, decreased gradually when the applied potentials increased positively from 0 to 1.15 V, and two new bands grew up at 390 and 781 nm due to the more planar TPA radical cation resonance structures after an electron removal from the lone pair on the nitrogen atom of the TPA moiety, thus shifted the absorption to longer wavelength. The UV–vis–NIR absorption changes in the polyamide **Ib** film at various potentials were fully reversible associated with strong color changes. The other polyamides showed similar spectral change to that of **Ib**. From the inset shown in Figure 7, the polyamide **Ib** film switches from highly transmissive neutral state (colorless: L^*, 99; a^*, 0; and b^*, 0) to a coloring oxidized state (deep bluish-green: L^*, 50; a^*, -24; and b^*, -4). The colorations were homogeneously distributed across the polymer film and survived for more than hundreds of redox cycles. Polyamide **Ib** exhibited high contrast of optical transmittance change ($\Delta T\%$) up to 87% at 781 nm and 54% at 390 nm. The absence of

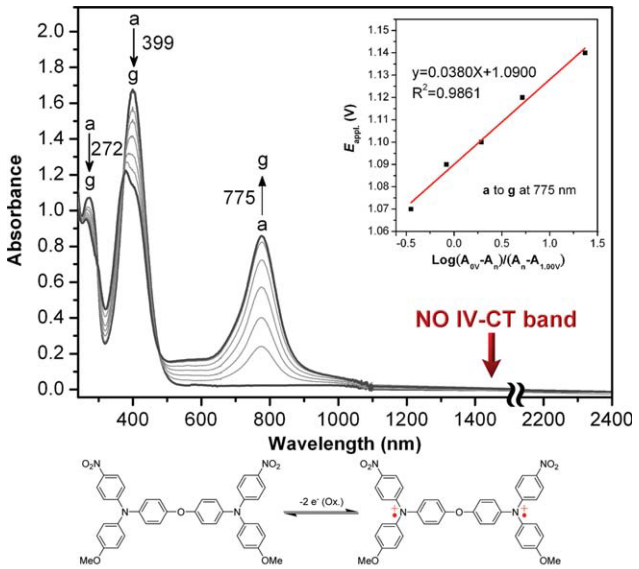

FIGURE 6 Absorption spectral change of dinitro compound **2** (5×10^{-4} M) in 0.1 M TBAP/CH_3CN at $E_{applied}$ of (a) 0, (b) 1.07, (c) 1.09, (d) 1.10, (e) 1.12, (f) 1.14, and (g) 1.18 (V vs. Ag/AgCl) and the oxidation pathway. [Color figure can be viewed in the online issue, which is available at wileyonlinelibrary.com.]

IV-CT band in the TPAO-based polymers was confirmed because of the introduction of ether-linkage, which was demonstrated by the spectroelectrochemical investigation of model compound **2**.

The color switching times were estimated by chronoamperometric and absorbance measurements (Supporting Information Fig. S12). The switching time was calculated at 90% of the full switch because it is difficult to perceive any further color change with naked eye beyond this point. As depicted in Supporting Information Figure S12, when the potential was switched between 0 and 0.99 V, polyamide **Ib** thin film revealed switching time of 3.14 s for coloring and 1.04 s for bleaching process. As depicted in Figure 8, the EC stability of the polyamide **Ib** film was determined by measuring the optical changes as a function of the number of switching cycles and plotted every 10th cycle. The EC CE ($\eta = \delta OD/Q$) and injected charge (electroactivity) after various switching steps were monitored and are summarized in Supporting Information Table S4. The EC film of **Ib** was found to exhibit high CE up to 166 cm^2/C at 781 nm, and showed only 4.8% decay of its electroactivity after 100 cycles (Fig. 8).

Furthermore, a single layer EC cell was fabricated as preliminary investigation (Fig. 9). The polyamide films were spray-coated onto ITO-glass and then dried. Afterward, the gel electrolyte was spread on the polymer-coated side of the electrode and the electrodes were sandwiched. To prevent leakage, an epoxy resin was applied to seal the device. As a typical example, an EC cell based on polyamide **Ib** was fabricated. The polymer film is colorless in neutral form. When the voltage was increased (to a maximum of 1.0 V), the color changed to bluish-green due to electro-oxidation, the same as that was already observed for the solution spectroelectrochemical experiments. When the potential was subsequently set back at 0 V, the polymer film turned back to original colorless. We believe that optimization could further improve the device performance and fully explore the potential of these EC polyamides.

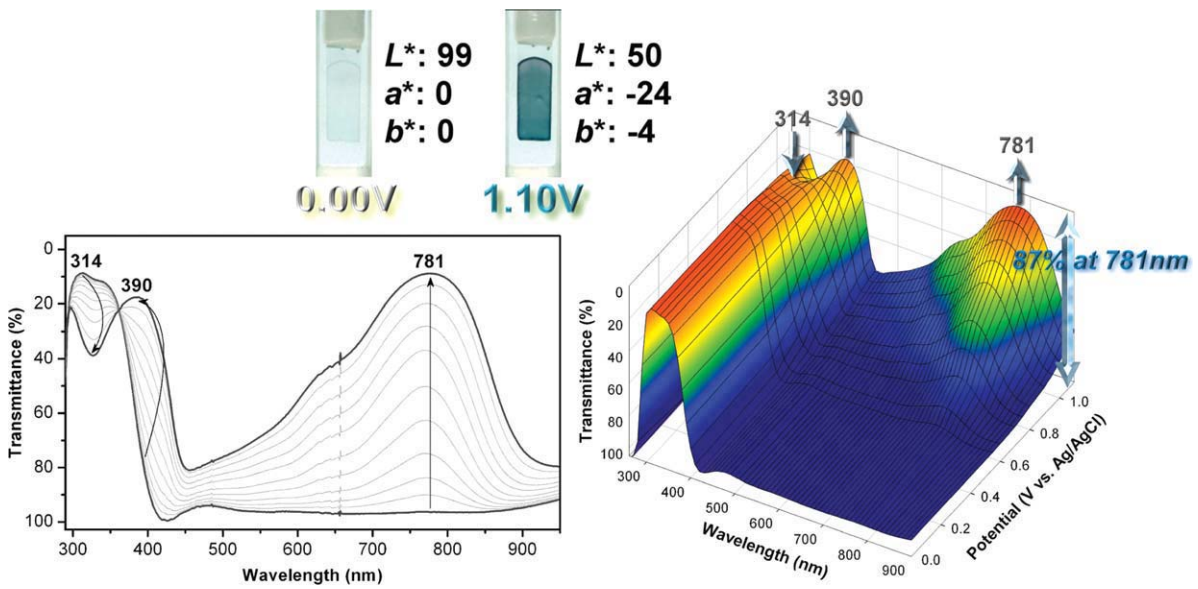

FIGURE 7 EC behavior (left) by increasing the applied voltage to 1.10 (V vs. Ag/AgCl), and 3D spectroelectrochemical behavior (right) from 0.00 to 1.10 (V vs. Ag/AgCl) of polyamide **Ib** thin film (~70 nm in thickness) on the ITO-coated glass substrate in 0.1 M TBAP/CH_3CN. The potential was varied in 50 mV interval. The inset shows the color change of the polymer film at indicated potentials. [Color figure can be viewed in the online issue, which is available at wileyonlinelibrary.com.]

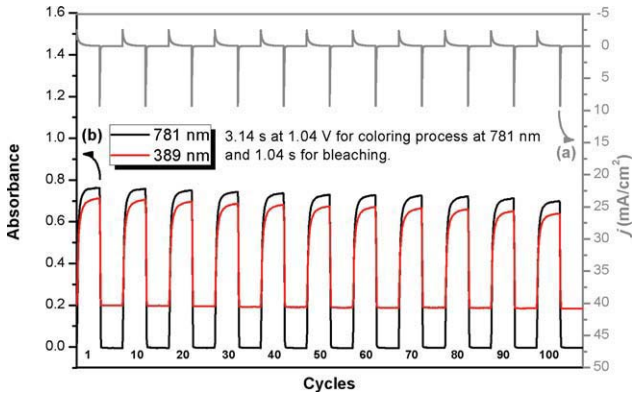

FIGURE 8 EC switching between 0 and 0.99 V (vs. Ag/AgCl) of polyamide **Ib** thin film (~80 nm in thickness) on the ITO-coated glass substrate (coated area: 1.6 cm × 0.6 cm) in 0.1 M TBAP/CH_3CN with a cycle time of 40 s. (a) Current consumption and (b) absorbance change monitored at the given wavelength. [Color figure can be viewed in the online issue, which is available at wileyonlinelibrary.com.]

CONCLUSIONS

A series of anodic bluish-green EC polyamides with MV Class I transition have been readily prepared from the diamine, bis(*N*-4-aminophenyl-*N*-4-methoxyphenyl-4-aminophenyl)ether (**3**), and various dicarboxylic acids via direct phosphorylation polycondensation. In addition to the good solubility and high thermal stability, these anodically polymeric EC materials also revealed highly continuous cyclic stability of EC characteristics with good CE, changing color from the colorless to bluish-green after oxidized. Spectroelectrochemical investigations also demonstrated that these polymers can be used as potential anodic coloring materials in the development of EC devices.

By the introduction of ether-linkage into TPAO unit, the resulting polymers containing two separated redox centers revealed independent electrochemical behavior, and two electrons within TPAO moiety are simultaneously removed to form two radical cations without intramolecular ET. The confirmation of lacking electron coupling was further demonstrated by OTTLE measurements of model compounds by Nernst equation. The MV Class I/II/III transition and electrochemistry of bridged triarylamines were investigated in the aspect of small molecule and polymer systems.

EXPERIMENTAL

Materials

N,*N*′-Bis(4-aminophenyl)-*N*,*N*′-di(4-methoxylphenyl)-1,4-phenylenediamine (**M1**)[8(e)] and *N*,*N*′-bis(4-aminophenyl)-*N*,*N*′-di(4-methoxylphenyl)-4,4′-biphenyldiamine (**M2**)[8(g)] were synthesized according to a previously reported procedure. Commercially available dicarboxylic acids such as *trans*-1,4-cyclohexanedicarboxylic acid (**3a**), 4,4′-oxydibenzoic acid (**3b**), and 2,2′-bis(4-carboxyphenyl)hexafluoropropane (**3c**) were purchased from Tokyo Chemical Industry and used as received. Commercially obtained anhydrous calcium chloride ($CaCl_2$) was dried under vacuum at 180 °C for 8 h. TBAP was obtained from ACROS and recrystallized twice by ethyl acetate under nitrogen atmosphere and then dried *in vacuo* before use. All other reagents were used as received from commercial sources.

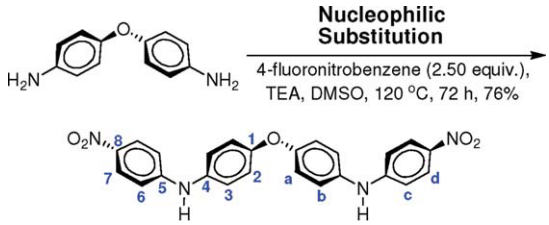

Bis(*N*-4-nitrophenyl-4-aminophenyl)ether (1)

A mixture of 9.20 g (90.92 mmol) of triethylamine in 80 mL DMSO was stirred at room temperature. To the mixture, 6.01 g (30.01 mmol) of 4,4′-oxydianiline and 10.72 g (75.21 mmol) of 4-fluoronitrobenzene were added in sequence. The mixture was heated with stirring at 120 °C for 72 h. The mixture was poured into stirred methanol/water, and the precipitated orange-red powders was collected by filtration and washed thoroughly with methanol/water (1:2). The product was filtered to afford 10.14 g (76% in yield) of orange-red powders with a mp of 103–106 °C (measured by DSC at 10 °C/min; ref. [13]; 163 °C).

FTIR (KBr): 3328 cm^{-1} (secondary N—H stretch), 1586 and 1312 cm^{-1} (—NO_2 stretch). ^1H NMR (500 MHz, DMSO-d_6, δ, ppm): 9.27 (s, 2H, —NH), 8.08 (d, 4H, J = 9.3 Hz, H_d), 7.28 (d, J = 8.9 Hz, 4H, H_a), 7.08 (d, J = 8.9 Hz, 4H, H_b), 7.01 (d, J = 9.3 Hz, 4H, H_c). ^{13}C NMR (125 MHz, DMSO-d_6, δ, ppm):

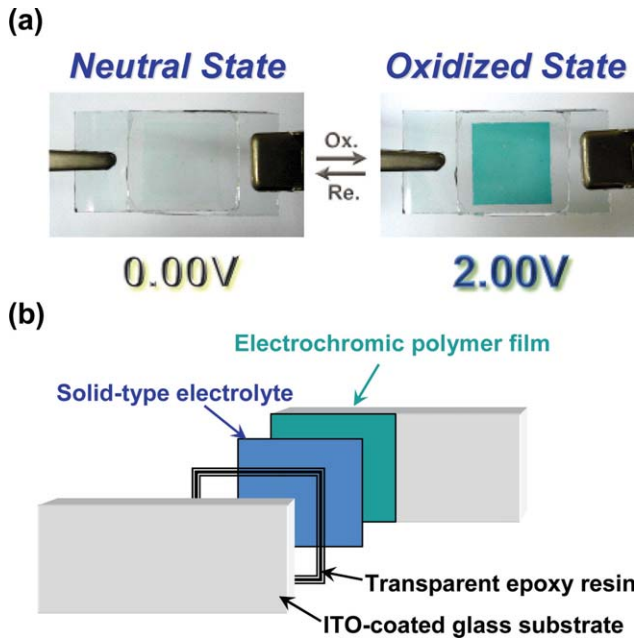

FIGURE 9 (a) Photographs of single-layer ITO-coated glass EC device, using polyamide **Ib** as active layer. (b) Schematic diagram of polyamide EC device sandwich cell.

152.9 (C^5), 151.2 (C^1), 137.5 (C^8), 135.3 (C^4), 126.2 (C^7), 123.2 (C^3), 119.5 (C^6), 112.8 (C^2).

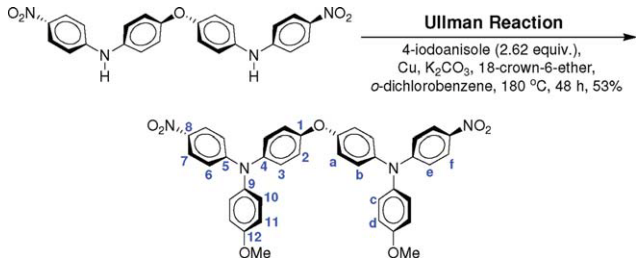

Bis(*N*-4-methoxyphenyl-*N*-4-nitrophenyl-4-aminophenyl) ether (2)

To a solution of 27.48 g (62.11 mmol) of dinitro compound **1**, 30.53 g (130.45 mmol) of 4-iodoanisole, 22.56 g (163.23 mmol) of powdered anhydrous potassium carbonate, 10.10 g (158.93 mmol) of copper powder, and 5.11 g (19.33 mmol) of 18-crown-6-ether were stirred in 105 mL of *o*-dichlorobenzene under nitrogen atmosphere. After heated at 180 °C for 48 h, the solution was filtered and poured into 1000 mL of MeOH. The precipitated brown powder was collected by filtration and purified by DMF/ethyl acetate. The product was filtered to afford 21.47 g (53% in yield) of bright yellow powder with a mp of 193–194 °C (measured by DSC at 10 °C/min).

FTIR (KBr): 1586, 1314 cm^{-1} (—NO_2 stretch). ^1H NMR (500 MHz, DMSO-d_6, δ, ppm): 8.04 (d, J = 9.4 Hz, 4H, H_f), 7.34 (d, J = 8.9 Hz, 4H, H_a), 7.28 (d, J = 8.9 Hz, 4H, H_c), 7.13 (d, J = 8.9 Hz, 4H, H_b), 7.04 (d, J = 8.9 Hz, 4H, H_d), 6.71 (d, J = 9.4 Hz, 4H, H_e), 3.78 (s, 6H, —OCH_3). ^{13}C NMR (125 MHz, DMSO-d_6, δ, ppm): 157.70 (C^{12}), 154.37 (C^1), 153.80 (C^8), 140.31 (C^5), 138.14 (C^9), 137.30 (C^4), 128.95 (C^{10}), 128.58 (C^2), 125.59 (C^7), 120.15 (C^3), 115.47 (C^{11}), 115.07 (C^6), 55.29 (—OCH_3). Anal. Calcd (%) for $C_{38}H_{30}N_4O_7$ (654.67): C, 69.72; H, 4.62; N, 8.56. Found: C, 69.70; H, 4.60; N, 8.74. Electron impact mass spectrometry (EI-MS): Calcd for $(C_{21}H_{19}N_3O_4)^+$, m/z 654.67; found, m/z 654.20.

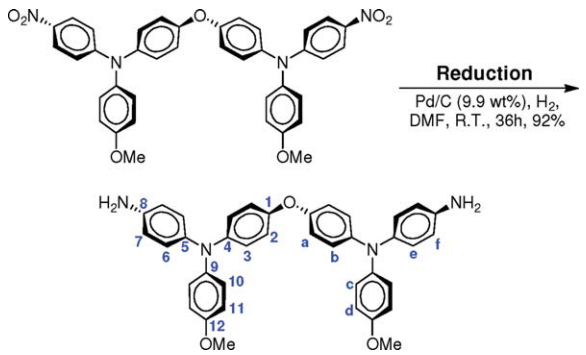

Bis(*N*-4-aminophenyl-*N*-4-methoxyphenyl-4-aminophenyl) ether (3)

In a 100-mL two-neck round-bottomed flask equipped with a stirring bar, 3.03 g (4.63 mmol) of dinitro compound **2** and 0.30 g of 10% Pd/C were dispersed in 42 mL of DMF, and the mixture was stirred vigorously under hydrogen atmosphere at room temperature until the theoretical amount of hydrogen was consumed. The time to reach this stage is about 36 h. The mixture was filtered to remove Pd/C, and the filtrate was poured into 300 mL of water and washed by MeOH. The precipitated product was collected by filtration and dried *in vacuo* at 65 °C to give 2.80 g (92% in yield) of grayish powder with a mp of 83–86 °C (measured by DSC of 10 °C/ min).

FTIR (KBr): 3443, 3365 cm^{-1} (N—H stretch). ^1H NMR (500 MHz, DMSO-d_6, δ, ppm): 6.91 (d, J = 9.0 Hz, 4H, H_a) , 6.84–6.80 (m, 8H, H_b + H_c), 6.78–6.75 (m, 8H, H_e + H_d), 6.54 (d, J = 8.8 Hz, 4H, H_f), 4.96 (s, 4H, —NH_2), 3.70 (s, 6H, —OCH_3). ^{13}C NMR (125 MHz, DMSO-d_6, δ, ppm): 154.51 (C^{12}), 150.47 (C^1), 145.42 (C^8), 144.30 (C^9), 141.19 (C^4), 136.07 (C^5), 126.91 (C^6), 124.49 (C^2), 121.16 (C^{11}), 118.94 (C^{10}), 114.84 (C^7), 114.55 (C^3), 55.10 (—OCH_3). Anal. Calcd (%) for $C_{38}H_{34}N_4O_3$ (594.70): C, 76.75; H, 5.76; N, 9.42. Found: C, 76.19; H, 6.00; N, 9.22. Electro-spray ionization mass spectrometry (ESI-MS): Calcd for $(C_{21}H_{23}N_3)^+$, m/z 594.70; found, m/z 594.60.

Polymer Synthesis

The synthesis of polyamide **Ib** was used as an example to illustrate the general synthetic route used to produce the polyamides. A mixture of 594.7 mg (1.00 mmol) of the diamine monomer (**2**), 258.2 mg (1.00 mmol) of 4,4′-oxydibenzoic acid (**4b**), 52.0 mg of calcium chloride, 0.90 mL of triphenyl phosphite, 0.50 mL of pyridine, and 0.8 mL of NMP was heated with stirring at 105 °C for 3 h. The obtained polymer solution was poured slowly into 300 mL of stirred water giving rise to a stringy, fiberlike precipitate that was collected by filtration, washed thoroughly with hot water and methanol, and dried under vacuum at 100 °C; yield: 829.0 mg (99%). Reprecipitations of the polymer by DMAc/methanol were carried out twice for further purification. The inherent viscosity and M_n of the obtained polyamide **Ib** were 0.51 dL/g (measured at a concentration of 0.5 g/dL in DMAc at 30 °C) and 134,800 Da, respectively.

The FTIR spectrum of **Ib** (film) exhibited characteristic amide absorption bands at 3317 cm^{-1} (N—H stretch), 3040 cm^{-1} (aromatic C—H stretch), 2928, 2829 cm^{-1} (CH_3 C—H stretch), 1649 cm^{-1} (amide carbonyl). ^1H NMR (500 MHz, DMSO-d_6, δ, ppm): 10.14 (s, 2H, —NH), 8.00 (d, J = 8.0 Hz, 4H, H_g), 7.63 (s, J = 8.4 Hz, 4H, H_a), 7.16 (d, J = 8.0 Hz, 4H, H_h), 7.00–6.90 (m, 20H), 3.72 (s, 6H, —OCH_3). ^{13}C NMR (125 MHz, DMSO-d_6, δ, ppm): 164.18 (C=O), 158.48, 155.48, 151.67, 143.56, 143.23, 140.23, 133.47, 130.34, 129.87, 126.17, 123.91, 122.45, 121.56, 119.34, 118.30, 114.89, 55.14 (—OCH_3). Anal. Calcd (%) for $(C_{52}H_{40}N_4O_6)_n$ $(816.90)_n$: C, 76.45; H, 4.94; N, 6.86. Found: C, 75.04; H, 4.95; N, 6.85. The other polyamides were prepared by an analogous procedure.

Preparation of the Polyamide Films

A solution of the polymer was made by dissolving 0.8 g of the polyamide sample in 12 mL of DMAc. The homogeneous solution was poured into a 9-cm glass Petri dish, which was placed in a 70 °C oven for 12 h to remove most of the

solvent, and then the semidried film was further dried *in vacuo* at 160 °C for 8 h. The obtained films were about 60–80 μm in thickness and were used for solubility tests, and thermal analyses.

Fabrication of the EC Device

EC polymer films were prepared by dropping solutions of the polyamide **Ib** (4 mg/mL in DMAc) onto a ITO-coated glass substrate (20 mm × 30 mm × 0.7 mm, 50–100 Ω/square). The polymers were drop coated onto an active area (ca. 20 mm × 20 mm) then dried in vacuum. A gel electrolyte based on poly(methyl methacrylate) (PMMA) (Mw: 350,000) and $LiClO_4$ was plasticized with propylene carbonate to form a highly transparent and conductive gel. PMMA (3 g) was dissolved in dry acetonitrile (15 g), and $LiClO_4$ (0.3 g) was added to the polymer solution as a supporting electrolyte. Then, propylene carbonate (5 g) was added as plasticizer. The gel electrolyte was spread on the polymer-coated side of the electrode, and the electrodes were sandwiched. Finally, an epoxy resin was used to seal the device.

Measurements

FTIR spectra were recorded on a PerkinElmer Spectrum 100 Model FTIR spectrometer. Elemental analyses were run in a Heraeus VarioEL-III CHNS elemental analyzer. ^{1}H NMR spectra were measured on a Bruker AVANCE-500 FT-NMR using tetramethylsilane as the internal standard, and peak multiplicity was reported as follows: s, singlet; d, doublet. ESI-MS and EI-MS spectra were measured on JEOL JMS-700 and Finnigan TSQ 700 mass spectrometers, respectively. The inherent viscosities were determined at 0.5 g/dL concentration using Tamson TV-2000 viscometer at 30 °C. Gel permeation chromatographic (GPC) analysis was performed on a Lab Alliance RI2000 instrument (one column, MIXED-D from Polymer Laboratories) connected with one refractive index detector from Schambeck SFD Gmbh. All GPC analyses were performed using a polymer/DMF solution at a flow rate of 1 mL/min at 70 °C and calibrated with polystyrene standards. TGA was conducted with a PerkinElmer Pyris 1 TGA. Experiments were carried out on ~6–8-mg film samples heated in flowing nitrogen or air (flow rate = 20 cm^3/min) at a heating rate of 20 °C/min. DSC analyses were performed on a PerkinElmer Pyris 1 DSC at a scan rate of 20 °C/min in flowing nitrogen (20 cm^3/min). Electrochemistry was performed with a CH Instruments 612C electrochemical analyzer. Voltammograms are presented with the positive potential pointing to the left and with increasing anodic currents pointing downward. CV and DPV were conducted with the use of a three-electrode cell in which ITO (polymer films area ca. 0.5 cm × 1.1 cm) was used as a working electrode. A platinum wire was used as an auxiliary electrode. All cell potentials were taken by using a homemade Ag/AgCl, KCl (sat.) reference electrode. Spectroelectrochemical experiments were carried out in a cell built from a 1-cm commercial UV–vis cuvette using Hewlett-Packard 8453 UV–vis diode array and Hitachi U-4100 UV–vis–NIR spectrophotometer. The ITO-coated glass slide was used as the working electrode, a platinum wire as the counter electrode, and a Ag/AgCl cell as the reference electrode. CE (η) determines the amount of optical density change (δOD) at a specific absorption wavelength induced as a function of the injected/ejected charge (Q; also termed as electroactivity) which is determined from the *in situ* experiments. CE is given by the equation: $\eta = \delta OD/Q = \log[T_b/T_c]/Q$, where η (cm^2/C) is the CE at a given wavelength, and T_b and T_c are the bleached and colored transmittance values, respectively. The thickness of the polyamide thin films was measured by alpha-step profilometer (Kosaka Lab., Surfcorder ET3000). Colorimetric measurements were obtained by JASCO V-650 spectrophotometer and the results are expressed in terms of lightness (L^*) and color coordinates (a^* and b^*).

The authors gratefully acknowledge the support of this research through the Institute of Nuclear Energy Research, Atomic Energy Council and the National Science Council (NSC98-2113-M-002-005-MY3) of Taiwan. C. W. Lu at the Instrumentation Center, National Taiwan University, for CHNS (EA) analysis experiments and C. H. Ho at the Instrumentation Center, Department of Chemistry, National Taiwan Normal University, for the measurement of 500 MHz NMR spectrometer are also acknowledged.

REFERENCES AND NOTES

1 (a) Monk, P. M. S.; Mortimer, R. J.; Rosseinsky, D. R. Electrochromism and Electrochromic Devices; Cambridge University Press: Cambridge, UK, 2007; (b) Mortimer, R. J. Chem Soc Rev 1997, 26, 147–156; (c) Rosseinsky, D. R.; Mortimer, R. J. Adv Mater 2001, 13, 783–793; (d) Somani, P. R.; Radhakrishnan, S. Mater Chem Phys 2003, 77, 117–133; (e) Liu, S.; Kurth, D. G.; Mohwald, H.; Volkmer, D. Adv Mater 2002, 14, 225–228; (f) Zhang, T.; Liu, S.; Kurth, D. G.; Faul, C. F. J. Adv Funct Mater 2009, 19, 642–652; (g) Maier, A.; Rabindranath, A. R.; Tieke, B. Adv Mater 2009, 21, 959–963; (h) Motiei, L.; Lahav, M.; Freeman, D.; van der Boom, M. E. J Am Chem Soc 2009, 131, 3468–3469; (i) Beaujuge, P. M.; Reynolds, J. R. Chem Rev 2010, 110, 268–320.

2 (a) Green, M. Chem Ind 1996, 17, 641–644; (b) Bach, U.; Corr, D.; Lupo, D.; Pichot, F.; Ryan, M. Adv Mater 2002, 14, 845–848; (c) Ma, C.; Taya, M.; Xu, C. Polym Eng Sci 2008, 48, 2224–2228; (d) Beaupre, S.; Breton, A. C.; Dumas, J.; Leclerc, M. Chem Mater 2009, 21, 1504–1513.

3 (a) Sonmez, G.; Meng, H.; Wudl, F. Chem Mater 2004, 16, 574–580; (b) Wang, S.; Todd, E. K.; Birau, M.; Zhang, J.; Wan, X.; Wang, Z. Y. Chem Mater 2005, 17, 6388–6394; (c) Qiao, W.; Zheng, J.; Wang, Y.; Zheng, Y.; Song, N.; Wan, X.; Wang, Z. Y. Org Lett 2008, 10, 641–644; (d) Zheng, J.; Qiao, W.; Wan, X.; Gao, J. P.; Wang, Z. Y. Chem Mater 2008, 20, 6163–6168; (e) Hasanain, F.; Wang, Z. Y. Dyes Pigments 2009, 83, 95–101.

4 Robin, M.; Day, P. Adv Inorg Radiochem 1967, 10, 247–422.

5 (a) Creutz, C.; Taube, H. J Am Chem Soc 1973, 95, 1086–1094; (b) Leung, M. K.; Chou, M. Y.; Su, Y. O.; Chiang, C. L.; Chen, H. L.; Yang, C. F.; Yang, C. C.; Lin, C. C.; Chen, H. T. Org Lett 2003, 5, 839–842.

6 Szeghalmi, A. V.; Erdmann, M.; Engel, V.; Schmitt, M.; Amthor, S.; Kriegisch, V.; Noll, G.; Stahl, R.; Lambert, C.; Leusser, D.; Stalke, D.; Zabel, M.; Popp, J. J Am Chem Soc 2004, 126, 7834–7845.

7 Lambert, C.; Nöll, G. J Am Chem Soc 1999, 121, 8434–8442.

8 (a) Liou, G. S.; Hsiao, S. H.; Su, T. X. J Mater Chem 2005, 15, 1812–1820; (b) Chang, C. W.; Liou, G. S. J Mater Chem 2008, 18, 5638–5646; (c) Chang, C. W.; Chung, C. H.; Liou, G. S. Macromolecules 2008, 41, 8441–8451; (d) Liou, G. S.; Chang, C. W. Macromolecules 2008, 41, 1667–1673; (e) Yen, H. J.; Liou, G. S. Chem Mater 2009, 21, 4062–4070; (f) Yen, H. J.; Lin, H. Y.; Liou, G. S. Chem Mater 2011, 23, 1874–1882; (g) Yen, H. J.; Lin, K. Y.; Liou, G. S. J Mater Chem 2011, 21, 6230–6237.

9 (a) Liou, G. S.; Lin, K. H. J Polym Sci Part A: Polym Chem 2009, 47, 1988–2001; (b) Kung, Y. C.; Liou, G. S.; Hsiao, S. H. J Polym Sci Part A: Polym Chem 2009, 47, 1740–1755; (c) Hsiao, S. H.; Liou, G. S.; Kung, Y. C.; Chang, Y. M. J Polym Sci Part A: Polym Chem 2010, 48, 2798–2809; (d) Hsiao, S. H.; Liou, G. S.; Kung, Y. C.; Hsiung, T. J. J Polym Sci Part A: Polym Chem 2010, 48, 3392–3401; (e) Huang, L. T.; Yen, H. J.; Chang, C. W.; Liou, G. S. J Polym Sci Part A: Polym Chem 2010, 48, 4747–4757; (f) Wang, H. M.; Hsiao, S. H.; Liou, G. S.; Sun, C. H. J Polym Sci Part A: Polym Chem 2010, 48, 4775–4789; (g) Yen, H. J.; Guo, S. M.; Liou, G. S. J Polym Sci Part A: Polym Chem 2010, 48, 5271–5281.

10 (a) Yamazaki, N.; Higashi, F.; Kawabata, J. J Polym Sci: Polym Chem Ed, 1974, 12, 2149–2154; (b) Yamazaki, N.; Matsumoto, M.; Higashi, F. J Polym Sci: Polym Chem Ed 1975, 13, 1375–1380.

11 Chang, C. W.; Liou, G. S.; Hsiao, S. H. J Mater Chem 2007, 17, 1007–1015.

12 (a) Murray, R. W.; Heineman, W. R.; O'Dom, G. W. Anal Chem 1967, 39, 1666–1668; (b) Yildiz, A.; Kissinger, P. T.; Reilley, C. N. Anal Chem 1968, 40, 1018–1024; (c) Heineman, W. R.; Norris, B. J.; Goelz, J. F. Anal Chem 1975, 47, 79–84.

13 Lecher, H. Z.; Parker, R. P.; Denton, J. J. U.S. Patent 2,385,088, 1944.